CAPABILITIES AND LIMITATIONS OF MONO-CAMERA PEDESTRIAN-BASED AUTOCALIBRATION

Raúl Mohedano and Narciso García

Grupo de Tratamiento de Imágenes, Universidad Politécnica de Madrid, 28040, Madrid, Spain
{rmp,narciso}@gti.ssr.upm.es; www.gti.ssr.upm.es

ABSTRACT

Many environments lack enough architectural information to allow an autocalibration based on features extracted from the scene structure. Nevertheless, the observation over time of walking people can generally be used to estimate the vertical vanishing point and the horizon line in the acquired image. However, this information is not enough to allow the calibration of a general camera without presuming excessive simplifications.

This paper presents a study on the capabilities and limitations of the mono-camera calibration methods based solely on the knowledge of the vertical vanishing point and the horizon line in the image. The mathematical analysis sets the conditions to assure the feasibility of the mono-camera pedestrian-based autocalibration. In addition, examples of applications are presented and discussed.

Index Terms— Camera calibration, vanishing point, horizon line, human tracking.

1. INTRODUCTION

Calibration of cameras is a very important field in computer vision, as the precise knowledge of the relation between real world coordinates and camera view observations can greatly improve many visual tasks of special interest, such as automatic scene modeling [1] or robust tracking systems [2].

It is desirable, for calibration purposes, to estimate three vanishing points corresponding to three mutually orthogonal directions of the real world [3]. This is practically achievable if the architecture of the observed scene is highly structured [4]. However, in many situations, the observed scene is not regularly structured. In these situations, we can use the observation over time of walking people to infer geometric information of the scene. Unfortunately, the information that can be extracted from pedestrians is not as accurate or complete as that estimated from structured architectures.

Walking people are usually modeled in the literature as vertical poles with constant height [5, 6, 7]. Under this hypothesis, it is possible to identify the vertical vanishing point in the image. Most works addressing mono-camera calibration assume, additionally, that people move on a regular and horizontal ground plane [5, 6, 8]. This makes it possible to assert that all the vanishing points detected by intersecting head-to-head and foot-to-foot lines lie on the same line: the horizon line.

There are excellent papers using vertical vanishing point and horizon line to calibrate a single camera. In [5], where no simplifications of the matrix K of intrinsic camera parameters are assumed, two orthogonal directions should be externally added to proceed. In [6], no external information about orthogonality is required. However, it assumes that the focal distance f is the only unknown intrinsic parameter, which seems too restrictive. Other works make additional assumptions for the pedestrian movement to improve the estimations, or to relax the assumptions for the matrix K. For example, [8] assume that pedestrians move at constant velocity. However, these assumptions do not seem to hold in general real situations.

Therefore, this paper studies the real capabilities and limitations of the automatic mono-camera calibration from pedestrian observation over time, with the only assumption that observed people walk on a regular, visible horizontal ground plane. We assume that it is possible to automatically estimate the vertical vanishing point $\mathbf{v}_{\mathrm{K}}$ and the horizon line $\mathbf{h}_{\mathrm{K}}$ from their tracks over time. This assumption is completely reasonable, as several works in the literature propose methods to achieve it [5, 6]. We discuss whether these data may allow to calibrate a general camera (with unknown focal distance, aspect ratio and principal point, but assuming that the skew can be discarded in practice), and under which circumstances.

2. PROJECTION OF THE VERTICAL VANISHING POINT AND THE HORIZON LINE

Let us begin reviewing the projection process for both the vertical vanishing point and the horizontal vanishing line. Although the complete projection matrix is $\mathrm{P} = \mathrm{K}\,\mathrm{R}\,[\,\mathrm{I}\,|-\mathrm{C}\,]$, where R represents the rotation and C the position of the camera into the world reference coordinate system, the projections of points at the infinity are not affected at all by this finite translation. Instead, we can treat them as spatial orientations or points of the projective plane $\mathbb{P}^2$. Thus, the projection of a certain direction of the space will be the subsequent application of two homographies, R and K, on the point of $\mathbb{P}^2$ it represents. In the following discussions, vectors in $\mathbb{R}^3$ will be denoted with circumflexed bold letters (*e.g.* $\hat{\mathbf{q}}$), whereas the point of $\mathbb{P}^2$ they determine will be denoted without circumflex (*e.g.* $\mathbf{q}$).

The vertical direction is represented in the real world coordinate system by $\hat{\mathbf{e}}_3$, which determines the point $\mathbf{e}_3$ of $\mathbb{P}^2$. The horizon line is determined by the vector plane generated by $\hat{\mathbf{e}}_1$ and $\hat{\mathbf{e}}_2$, so its dual projective representation coincide with the projective point determined by $\hat{\mathbf{e}}_3$, which is also the point $\mathbf{e}_3$, but now in $(\mathbb{P}^2)^*$. As explained in [9], if a projective space undergoes a transformation H, its dual space is transformed according to $\mathrm{H}^{-\mathrm{T}}$. Then, as $\mathrm{R}^{-\mathrm{T}} = \mathrm{R}$, the vertical vanishing point and the (dual of the) horizon line in the camera coordinate system centered at the optical axis are

$$\begin{array}{l} \hat{\mathbf{v}}_{\mathrm{R}} \propto \mathrm{R}\,\hat{\mathbf{e}}_3 = \hat{\mathbf{r}}_3 \\ \hat{\mathbf{h}}^*_{\mathrm{R}} \propto \mathrm{R}^{-\mathrm{T}}\,\hat{\mathbf{e}}_3 = \mathrm{R}\,\hat{\mathbf{e}}_3 = \hat{\mathbf{r}}_3 \end{array} \quad , \tag{1}$$

This work has been partially supported by the Ministerio de Ciencia e Innovación of the Spanish Government under project TEC2007-67764 (SmartVision). Also, R. Mohedano wishes to thank the Comunidad de Madrid for a personal research grant.

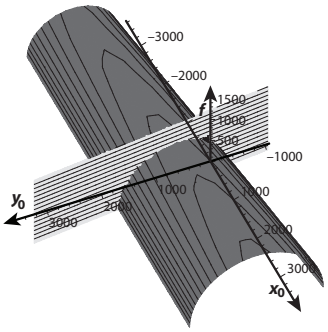

Fig. 1. Solution surfaces (only $f \geq 0$) for Eq. (5) (dark grey) and Eq. (7) (light grey) for a particular case ($f = 837.85$, $a = 1$, $x_0 = 258$, $y_0 = 204$, $\theta = -116^\circ$ and $\rho = -6.5^\circ$).

where $\hat{\mathbf{r}}_3$ is the third column of the rotation matrix R. Thus, in the camera normalized coordinate system (before applying K), the vertical vanishing point and the dual of the horizon line coincide at $\mathbf{r}_3$.

However, the effect of the matrix K is different. As $\mathrm{K}^{-\mathrm{T}} \neq \mathrm{K}$, the vertical vanishing point and the dual of the horizon line are respectively observed at

$$\begin{array}{l} \hat{\mathbf{v}}_\mathrm{K} \propto \mathrm{K}\,\hat{\mathbf{v}}_\mathrm{R} = \mathrm{K}\,\hat{\mathbf{r}}_3 \\ \hat{\mathbf{h}}^*_\mathrm{K} \propto \mathrm{K}^{-\mathrm{T}}\,\hat{\mathbf{h}}^*_\mathrm{R} = \mathrm{K}^{-\mathrm{T}}\,\hat{\mathbf{r}}_3 \end{array} \quad . \tag{2}$$

Thus, the projective points $\mathbf{v}_\mathrm{K}$ and $\mathbf{h}^*_\mathrm{K}$ observed in the pixel camera coordinate system do not coincide.

3. CAMERA PARAMETER RELATION WITH OBSERVED VERTICAL VANISHING POINT AND HORIZON

As explained before, the vertical vanishing point $\mathbf{v}_\mathrm{K}$ and the dual of the observed horizon line $\mathbf{h}^*_\mathrm{K}$ observed in the pixel camera coordinate system do not coincide in general because of the effect of the affine transform K. However, they will exactly coincide if we could compensate the effect of K. Let us assume a camera with zero skew and certain pixel aspect ratio a. Then, we have

$$\mathrm{K} = \begin{bmatrix} af & 0 & x_0 \\ 0 & f & y_0 \\ 0 & 0 & 1 \end{bmatrix} . \tag{3}$$

Note that, although it is common to include the aspect ratio term in the y direction [5], we consider it in the x direction as it helps to interpret the subsequent results. Undoing the K homography, and bearing in mind that both $\mathbf{v}_\mathrm{R}$ and $\mathbf{h}^*_\mathrm{R}$ coincide with $\mathbf{r}_3$, we have

$$\begin{array}{l} \hat{\mathbf{r}}_3 \propto \mathrm{K}^{-1}\,\hat{\mathbf{v}}_\mathrm{K} \\ \hat{\mathbf{r}}_3 \propto \mathrm{K}^{\mathrm{T}}\,\hat{\mathbf{h}}^*_\mathrm{K} \end{array} \quad \Rightarrow \quad \mathrm{K}^{-1}\,\hat{\mathbf{v}}_\mathrm{K} \propto \mathrm{K}^{\mathrm{T}}\,\hat{\mathbf{h}}^*_\mathrm{K} \,. \tag{4}$$

Two vectors are linearly dependent if and only if their cross product is zero. Then, assuming $\hat{\mathbf{v}}_\mathrm{K} = [x_V, y_V, \alpha_V]^\mathrm{T}$ and $\hat{\mathbf{h}}^*_\mathrm{K} = [x_H, y_H, \alpha_H]^\mathrm{T}$, this condition yields the three equations

$$(\alpha_V y_H)(f)^2 = (y_V - \alpha_V y_0)(x_H x_0 + y_H y_0 + \alpha_H) \tag{5}$$

$$(\alpha_V x_H)(af)^2 = (x_V - \alpha_V x_0)(x_H x_0 + y_H y_0 + \alpha_H) \tag{6}$$

$$y_H(x_V - \alpha_V x_0) = a^2 x_H (y_V - \alpha_V y_0) \,. \tag{7}$$

It can be seen that if two of these equations are satisfied, then the remaining equation holds automatically, unless these two equations have degenerated into the same condition.

In order to analyze the solutions of this system of equations, we should distinguish, in practice, three different situations:

- $\alpha_V \neq 0$ and $x_H^2 + y_H^2 \neq 0$
- $\alpha_V = 0$
- $x_H^2 + y_H^2 = 0$

In the first case, more general and common in real situations, vertical lines are perceived as convergent, and the horizon line does lie on the affine image plane. The other two cases are actually mutually exclusive, as we will prove in Section 4, and are not common in real settings. However, they are worth studying separately, at least at limit degenerate cases of the general one.

3.1. General case: $\alpha_V \neq 0$ and $x_H^2 + y_H^2 \neq 0$

If $\alpha_V \neq 0$, and in addition x_H and y_H are not both zero, each of the Eqs. (5), (6) and (7) defines a surface of $\mathbb{R}^3$ (where each axis represent one of the unknowns: x_0, y_0 and f). Eq. (7) can be rewritten as

$$(\alpha_V y_H)x_0 - (\alpha_V a^2 x_H)y_0 + (a^2 x_H y_V - y_H x_V) = 0 \tag{8}$$

which shows that it is simply the equation of a line on the $\overrightarrow{x_0, y_0}$ plane. This restriction is satisfied by the observed vertical vanishing point $\mathbf{v}_\mathrm{K}$, which indicates that the principal point (x_0, y_0) must be located on a line passing through $\mathbf{v}_\mathrm{K}$ whose slope is determined by the aspect ratio a. In fact, the normal vector of this surface is $\mathbf{n}_3 = (y_H, -a^2 x_H, 0)$ or, restricting to the $\overrightarrow{x_0, y_0}$ plane, $\mathbf{n}_3 = (y_H, -a^2 x_H)$.

Eq. (7) can be seen as a simple restriction for the position of the principal point (x_0, y_0), whereas Eqs. (5) and Eq. (6) indicate which f satisfies the observed $\mathbf{v}_\mathrm{K}$ and $\mathbf{h}^*_\mathrm{K}$ for each valid principal point. If $y_H \neq 0$ (as we have assumed previously that $\alpha_V \neq 0$) then Eq. (5) define a conic surface. It is a really soft assumption in practice, as in common settings the horizon line is clearly perceived as horizontal, and thus $|y_H| \gg |x_H|$. As in that case Eqs. (5) and (7) do not degenerate into the same condition, they characterize completely the solutions of the system of equations.

Let us analyze, then, the main characteristics of the surface defined by Eq. (5) for $y_H \neq 0$: considering that f must be positive, and considering that $\alpha_V y_H \neq 0$, we can write

$$f = +\sqrt{\left(\frac{y_V}{\alpha_V} - y_0\right)\left(\frac{x_H x_0 + y_H y_0 + \alpha_H}{y_H}\right)} \,. \tag{9}$$

Here, the first factor inside the square root indicates the signed distance between (x_0, y_0) and the line $y_0 = y_V/\alpha_V$: in other words, it is the (signed) distance on the affine image plane between the principal point and the y coordinate of the observed vertical vanishing point. The latter factor is proportional to the signed distance between the principal point and the observed horizon line (also on the affine image plane). The first factor is positive towards the negative y_0 axis (and negative on the opposite half plane), whereas the latter undergoes the opposite effect (positive towards the positive y_0 axis and negative on the opposite half plane). As f is real and positive, the solution is only defined when the argument of the square root is positive, which happens if and only if both factors have the same sign. Thus there will only be valid solutions for Eq. (5) in the area comprised between both lines, restricting even more the range of possible positions of the principal point. In addition, both lines satisfy Eq. (5) for $f = 0$, so every cut of this conic surface will yield a convex curve. The typical shape of the surfaces defined by Eqs. (5) and (7) is shown in Fig. 1.

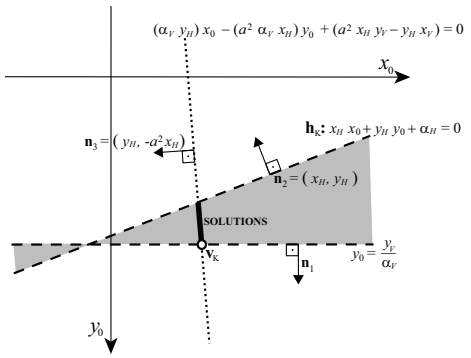

Fig. 2. Possible locations for the principal point (x_0, y_0) in the general case. The dotted line depicts Eq. (8) condition. The shaded area indicates the valid solutions for Eq. (9). The strongly marked segment marks the final range of possible positions of (x_0, y_0).

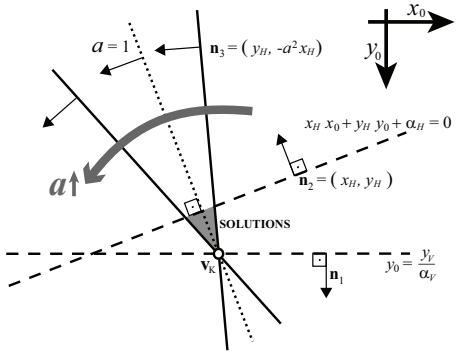

Fig. 3. Location of the possible real principal points (x_0, y_0) in the general case for a given range of aspect ratios (shaded area). The thick grey arrow indicates the variation of Eq. (8) as a increases.

To improve the perception of the results, all graphs presenting the solutions have been displayed with the axes x_0 and y_0 in the same orientation of that of x and y in the common pixel camera coordinate system, in which x points rightwards and y points downwards. The purpose of this choice is to identify easily lines and points of the solution space with lines and points observed on the affine image plane. However, all equations consider x_0 as the first variable and y_0 as the second one.

Thus, Eq. (9) decisively depends on two different lines that are both solutions of the equation for $f = 0$, and that are related to each of the multiplicative factors of the square root. The line $y_0 = y_V/\alpha_V$, which obviously pass through the observed vanishing point $\mathbf{v}_\mathrm{K}$, is orthogonal to the vector $\mathbf{n}_1 = (0, 1)$. The other, which is the observed horizon line, is orthogonal to the vector $\mathbf{n}_2 = (x_H, y_H)$. As $|y_H| \gg |x_H|$ in practice, both vectors are almost parallel, and so are the lines they define. Meanwhile, as discussed before, the principal point must lie on the line determined by Eq. (8), which is orthogonal to $\mathbf{n}_3 = (y_H, -a^2 x_H)$. The aspect ratio a is in practice positive and close to one, and therefore $\mathbf{n}_2$ and $\mathbf{n}_3$ are nearly perpendicular (and so are $\mathbf{n}_1$ and $\mathbf{n}_3$). This behavior is depicted in Fig. 2, that proves that the choice of Eqs. (5) and (7) facilitates the comprehension of the set of possible solutions in practical situations.

Until now, we have assumed a certain fixed aspect ratio a. However, it would be very interesting to study how different aspect ratio values affect the solutions of the equations. With the aspect ratio a as defined in Eq. (3), and using Eqs. (5) and (7) as explained before, a only affects the orientation of the line determined by Eq. (7), which passes always through the observed vertical vanishing point (which can be considered fixed data). This is clearly depicted in Fig. 3. As usual aspect ratios are close to one, and $a = 1$ implies that $\mathbf{n}_3$ is orthogonal to $\mathbf{n}_2$, probable solutions for Eq. (7) will form a limited pencil of lines around the line orthogonal to the observed horizon line (see Fig. 3). The typical shape of the whole set of possible solutions for a certain range of aspect ratios (around $a = 1$) is shown in Fig. 4.

Anyway, although assuming $y_H \neq 0$ is safe in practice (as discussed in Section 4), let us suppose that it is zero. The assumption of x_H and y_H not being zero simultaneously implies that if $y_H = 0$ then $x_H \neq 0$. In this situation, it suffices to study Eqs. (6) and (7) instead of Eqs. (5) and (7). This case is analogous to the previously detailed one, although less convenient in practice.

3.2. Limit cases

If any of the two conditions of the general case is not fulfilled, the system of equations degenerates and it is not possible to obtain any information about the focal distance f. Therefore, it is not possible to advance in the analysis of the matrix K.

3.2.1. Limit case 1: $\alpha_V = 0$

Our previous analysis of Eq. (5), conducted through its rewriting into Eq. (9), assumes $\alpha_V y_H \neq 0$. However, α_V can actually be zero in a particular setting, where the optical axis is completely parallel to the real world ground plane. Although this situation is not practical in many applications, it is possible, and interesting as a limit case.

The condition $\alpha_V = 0$ indicates that the vertical vanishing point is perceived as a point at the infinity, and thus that the real world vertical lines are perceived as parallel lines. In addition, $\alpha_V = 0$ also implies in practice that x_H and y_H are not both zero, as shown in Section 4. Now, in this situation, Eqs. (5), (6), and (7) degenerate into

$$y_V\,(x_H x_0 + y_H y_0 + \alpha_H) = 0 \tag{10}$$

$$x_V\,(x_H x_0 + y_H y_0 + \alpha_H) = 0 \tag{11}$$

$$y_H\, x_V = a^2\, x_H\, y_V\,. \tag{12}$$

As we have hypothesized that $\alpha_V = 0$, and given that $\hat{\mathbf{v}}_\mathrm{K}$ must define a projective point, then x_V and y_V cannot be zero simultaneously. Thus, Eqs. (10) and (11) can only be satisfied simultaneously if the principal point (x_0, y_0) is contained in the observed horizon line $\mathbf{h}^*_\mathrm{K}$. Additionally, Eq. (12) might be used to determine the aspect ratio (if unknown), unless x_V or y_V are zero. However, every clue about f is lost, avoiding any assertion about its value or even about its relation to the principal point.

3.2.2. Limit case 2: $x_H^2 + y_H^2 = 0$

As shown in Section 4, x_H and y_H can only be simultaneously zero in a very specific camera setting: optical axis completely perpendicular to the real world ground plane. It can be proved that, in addition, this setting ensures that $\alpha_V \neq 0$. In this situation, Eqs. (7) is always satisfied (becoming useless) and Eqs. (5) and (6) degenerate into

$$\alpha_H(y_V - \alpha_V y_0) = 0 \tag{13}$$

$$\alpha_H(x_V - \alpha_V x_0) = 0\,. \tag{14}$$

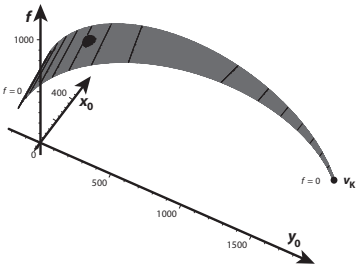

Fig. 4. Final solution surface for a particular case (same parameters as in Fig. 1), for aspect ratios in the range $[0.5, 1.5]$. The set of real intrinsic values (x0, y0 and f) is shown as a black point, that is effectively contained in the solution surface.

As we have presumed that x_H and y_H are both zero, and given that $\hat{\mathbf{h}}^*_{\mathrm{K}}$ must define a projective point, then α_H cannot be zero. Thus Eqs. (13) and (14) determine that the principal point is $(x_0, y_0) = \left(\frac{x_V}{\alpha_V}, \frac{y_V}{\alpha_V}\right)$. In other words, the principal point coincides with the observed vertical vanishing point. However, every clue about f and a is lost, making it impossible to infer their value or their possible valid ranges.

4. PARTICULARIZATION FOR REAL CAMERA SETTINGS

Until now, we have discussed the possible solutions for an arbitrary vertical vanishing point $\mathbf{v}_{\mathrm{K}}$ and horizon line $\mathbf{h}^*_{\mathrm{K}}$. However, in practice, the observed $\mathbf{v}_{\mathrm{K}}$ and $\mathbf{h}^*_{\mathrm{K}}$ are strongly related, and depends directly on the geometry and the intrinsic parameters of the camera. Let us discuss these relations.

As the perception of the real world vertical and the horizontal ground plane is not affected by the exact placement of the x and y axes on it, the rotation matrix R may only be parameterized using two angles: θ and ρ. The angle θ indicates the angle between the camera optical axis and the real world horizontal plane. Thus, as in usual geometrical settings the camera points slightly downwards, it is safe to assume that $-\pi/2 > \theta > -\pi$. The angle ρ determines the rotation of the camera around its optical axis. In practical situations, this angle is close to zero. Thus, matrix R can be written as

$$\mathrm{R} = \mathrm{R}_z(\rho)\,\mathrm{R}_x(\theta) = \\ = \begin{bmatrix} \cos\rho & -\sin\rho & 0 \\ \sin\rho & \cos\rho & 0 \\ 0 & 0 & 1 \end{bmatrix} \begin{bmatrix} 1 & 0 & 0 \\ 0 & \cos\theta & -\sin\theta \\ 0 & \sin\theta & \cos\theta \end{bmatrix}. \quad (15)$$

Thus, its third column is

$$\hat{\mathbf{r}}_3 = \begin{bmatrix} \sin\rho\,\sin\theta \\ -\cos\rho\,\sin\theta \\ \cos\theta \end{bmatrix}. \quad (16)$$

This means that the observed vertical vanishing point must be

$$\hat{\mathbf{v}}_{\mathrm{K}} \sim \mathrm{K}\,\hat{\mathbf{r}}_3 = \begin{bmatrix} af\sin\rho\,\sin\theta + x_0\cos\theta \\ -f\cos\rho\,\sin\theta + y_0\cos\theta \\ \cos\theta \end{bmatrix}. \quad (17)$$

The observed horizontal line is

$$\hat{\mathbf{h}}_{\mathrm{K}} \sim \mathrm{K}\,\hat{\mathbf{r}}_3 = \\ = \begin{bmatrix} (af)^{-1}\sin\rho\,\sin\theta \\ -(f)^{-1}\cos\rho\sin\theta \\ -(af)^{-1}\sin\rho\sin\theta + (f)^{-1}\cos\rho\sin\theta + \cos\theta \end{bmatrix}. \quad (18)$$

These results show that, in practice, $\alpha_V = \cos\theta$. Thus α_V can only be identically zero if $\theta = \pi/2$, implying that $|\sin\theta|$ is 1. As ρ is close to zero in practical settings, $\cos\rho$ is close to 1 and then y_H cannot be zero. Analogously, x_H and y_H can only be both zero if $\sin\theta = 0$. Then, $|\cos\theta| = 1$ and therefore α_V cannot be zero.

5. CONCLUSIONS

A study on the capabilities and limitations of mono-camera calibration methods based on the observation of walking people has been presented. These methods are mainly useful when the observed scene is not regularly structured or there is no recognizable architecture. That is, when the only available information can be extracted from the observation over time of walking people.

Under these conditions, only the estimation of the vertical vanishing point and the horizon line are feasible. The analysis carried out discusses whether the solely knowledge of these two data may allow to calibrate a general camera. So, we have considered cameras with unknown focal distance, aspect ratio, and principal point, only assuming that the skew can be discarded (usual assumption in practical situations).

A set of equations for the possible values of the intrinsic parameters have been derived. The general case has been identified, proving that the complete autocalibration cannot be achieved only from the vertical vanishing point and the horizon line. Nevertheless, the relations between the different intrinsic parameters have been established. Adding additional restrictions, the set of conditions to assure the feasibility of the mono-camera pedestrian-based autocalibration has been derived. In addition, simple but representative results have also been presented and discussed, allowing a visual interpretation of the above mentioned set of conditions.

6. REFERENCES

[1] E. Delage, H. Lee, and A. Y. Ng, "A dynamic bayesian network model for autonomous 3d reconstruction from a single indoor image," in *Proc. CVPR*, 2006, vol. 2, pp. 2418–2428.

[2] M. Isard and J. MacCormick, "Bramble: A bayesian multiple-blob tracker," in *Proc. IEEE ICCV*, 2001, pp. 34–41.

[3] G. Wang, H.-T. Tsui, and Q. M. J. Wu, "What can we learn about the scene structure from three orthogonal vanishing points in images," *Pattern Recognition Letters*, vol. 30(3), pp. 192–202, 2009.

[4] P. Denis, J. H. Elder, and F. J. Estrada, "Efficient edge-based methods for estimating manhattan frames in urban imagery," in *Proc. ECCV*, 2008, vol. 2, pp. 197–210.

[5] F. Lv, T. Zhao, and R. Nevatia, "Camera calibration from video of a walking human," *IEEE Trans. PAMI*, vol. 28, no. 9, pp. 1513–1518, 2006.

[6] N. Krahnstoever and P. R. S. Mendonça, "Bayesian autocalibration for surveillance," in *Proc. IEEE ICCV*, 2005, vol. 2, pp. 1858–1865.

[7] I. N. Junejo, "Using pedestrians walking on uneven terrains for camera calibration," *Machine Vision and Applications*, 2009.

[8] N. Krahnstoever and P. R. S. Mendonça, "Autocalibration from tracks of walking people," in *British Machine Vision Conference*, 2006, vol. 2, p. 107.

[9] R. I. Hartley and A. Zisserman, *Multiple View Geometry in Computer Vision*, Cambridge University Press, ISBN: 0521540518, second edition, 2004.